

## Observation of the second-harmonic generation from relativistically quivering electrons in exciting laser wakefield

Eiji Takahashi

*Center for Tsukuba Advanced Research Alliance, University of Tsukuba, 1-1-1 Tennodai, Tsukuba, Ibaraki, 305-8577, Japan and  
Energy and Environmental Science, Graduate School of Engineering, Utsunomiya University, 7-1-2 Yoto Utsunomiya,  
Tochigi, 321-8585, Japan*

Michiaki Mori

*Center for Tsukuba Advanced Research Alliance, University of Tsukuba, 1-1-1 Tennodai, Tsukuba, Ibaraki, 305-8577, Japan*

Noboru Yugami and Yasushi Nishida

*Energy and Environmental Science, Graduate School of Engineering, Utsunomiya University, 7-1-2 Yoto Utsunomiya,  
Tochigi, 321-8585, Japan*

Kiminori Kondo

*Center for Tsukuba Advanced Research Alliance, University of Tsukuba, 1-1-1 Tennodai, Tsukuba, Ibaraki, 305-8577, Japan*

(Received 4 January 2001; revised manuscript received 29 June 2001; published 13 December 2001)

The second-harmonic emission generated by the spatially asymmetric quivering electrons caused by the ponderomotive force was studied. The intensity of the second harmonic was proportional to the focused intensity of the pump pulse with the power of 1.8. This intensity dependence can be explained by the relativistic effect of the quivering electrons.

DOI: 10.1103/PhysRevE.65.016402

PACS number(s): 52.38.-r, 42.65.Dr, 42.65.Ky, 52.35.Mw

The interaction between an ultrashort high-peak power laser and plasmas is rich in a variety of interaction phenomena of high-intensity physics. A recent high-power laser technology has enabled the instantaneous power of 1 PW [1] in the single-shot base and 100 TW in 10 Hz [2]. If 1 PW pulse is focused to 10  $\mu\text{m}$  size, the peak intensity achieves to  $10^{21}$  W/cm<sup>2</sup>. In this region, the quiver energy  $U_p$  achieves to 100 MeV with 1  $\mu\text{m}$  in wavelength. The physics related to the fast ignitor (FI) concept [3] in inertial confinement fusion can be studied in this region with a special single-shot system. Even if 1 TW laser pulse focused to 10  $\mu\text{m}$  size, the peak intensity achieves to  $10^{18}$  W/cm<sup>2</sup>, which corresponds to the quiver energy of 0.1 MeV. The normalized vector potential field  $a_0$  achieves to  $\sim 1$ , because  $a_0 = 0.85\lambda\sqrt{I_0}$ . Here,  $\lambda$  is laser wavelength in units of  $\mu\text{m}$  and  $I_0$  is laser intensity in units of  $10^{18}$  W/cm<sup>2</sup>. Therefore, the relativistic effect starts to appear even in this region. The study of the interaction physics in this region also gives us important information not only for FI, but also for other interesting applications: for example, the laser accelerator [4] and the hard x-ray laser [5]. Especially in the application to laser accelerator, the plasma physics related to the laser wakefield has to be understood both experimentally and theoretically. Through this understanding process, control of the laser wakefield (LWF) and the long distance laser guiding has to be technically realized for the real laser accelerator [6].

In the study of the laser accelerator, the understanding of the excitation of the laser wakefield is one of the important issues. When the laser wakefield is excited, the laser intensity is high enough to induce the ponderomotive electron current towards outside of the focus in the standard-type laser wakefield (LWF), or induce the lateral plasma oscillation in self-modulated laser wakefield [7]. Both the plasma cur-

rent and the plasma oscillation in exciting LWF cause the spatially asymmetric nonlinear motion of the quivering electrons. Then the second-harmonic emission can be generated. However, the observation of the second-harmonic emission from the laser-produced plasmas was reported approximately 15 years ago [8,9] without using the chirped-pulse-amplification (CPA) laser [10]. In their studies, the focused laser intensity was so high that filamentation occurred. At the filaments, the steep spatial density gradient was formed, then the second-harmonic emission could be generated with a stimulated Brillouin backscattering. The observed second-harmonic emission was not really a harmonic, but rather a sum frequency of the forward and back-reflected light. In Refs. [7,11,12], the theoretical explanation was described. If the spatial distribution of the plasma density is uniform, not even harmonic emission is generated. But if the plasma has the initial spatial density gradient prior to the arrival of the pump pulse, a source current for the second-harmonic can be driven. In Ref. [13], the second harmonic emission of the side-scattered stimulated Raman scattered (SRS) light was observed. In their case, the side scattered SRS light of the fundamental pump pulse was frequency doubled at the steep radial density gradient by the ponderomotive electron cavitation. In Ref. [14], the fundamental pump pulse was frequency doubled at the edge of the pump pulse. After frequency doubling, that second-harmonic pulse was also scattered at the electron plasma wave (EPW), then the SRS signal of the second-harmonic emission was observed. In their case, frequency doubling occurred at the edge of the laser-produced plasma before Raman scattering.

In this paper, we observed the second-harmonic generation from the steep density gradient by the ponderomotive electron cavitation. The density of the plasma was set to be

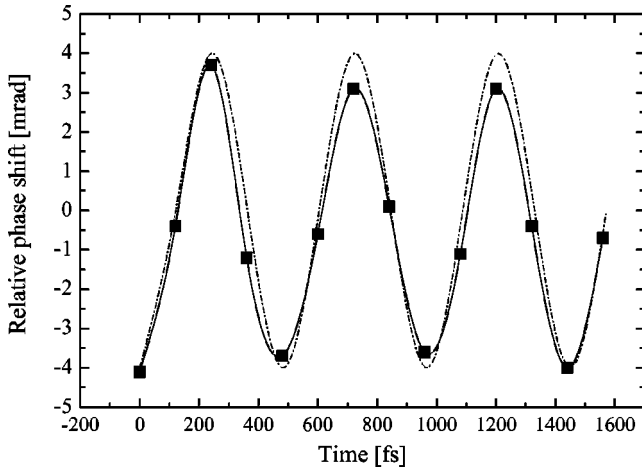


FIG. 1. Relative phase shift versus time delay. The gas pressure was 0.8 Torr in He. The laser intensity at the focal region was  $5 \times 10^{17}$  W/cm<sup>2</sup>. The dots correspond to the experimental data and the dash-dotted line corresponds to a numerical fit.

low enough that the oscillation period of the EPW was longer than the pulse width of the pump pulse. Then, no SRS process occurred. The focused laser intensity was estimated to be up to  $1.3 \times 10^{18}$  W/cm<sup>2</sup>, which corresponds to  $a_0 \sim 0.8$  at  $\lambda = 800$  nm. The second-harmonic intensity was not simply proportional to the square of the pump intensity, it was proportional to the pump intensity with the power of 1.8. This intensity dependence can be explained by the relativistic quiver motion of the electrons.

The experimental studies were carried out with a 10 Hz, TW-class Ti:sapphire laser system. In this system, the pulse width was 100 fs and the wavelength was centered at 800 nm. The pump pulse was focused by a CaF<sub>2</sub> planoconvex lens of  $f/4$  in the target chamber. The spot image of the pump pulse at the focal plane was measured to be  $8 \mu\text{m}$  full width at half maximum. Then, the peak intensity at the focus was estimated to be up to  $1.3 \times 10^{18}$  W/cm<sup>2</sup>. The target gas was helium, which filled the target chamber statically. The pump pulse ionized the helium gas near the focal region by the tunneling ionization. In this experiment, the density of the plasma was low enough that no defocus was thought to happen [15]. Then, the EPW of the LWF may be excited by the ponderomotive pressure.

To confirm the excitation of the EPW and its oscillation period, we first measured the temporal oscillation of the EPW using a frequency domain interferometry. Details of this measurement have been presented in a previous publication [16,17]. Typical measurement of the relative phase shift versus the time delay is shown in Fig. 1. In this measurement, the gas pressure was fixed to be 0.8 Torr in He and the electron plasma density  $n_e$  was estimated to be  $5.3 \times 10^{16}$  cm<sup>-3</sup>. The EPW oscillation period  $T_{pe}$  was evaluated to be 480 fs. The horizontal and vertical axes correspond to the time delay and the measured relative phase shift, respectively. The dots in Fig. 1 correspond to the experimentally obtained phase shift. The dash-dotted line is a numerical fit with  $T_{pe}$  of 480 fs. This experimental result pointed out that not only was the pump pulse really focused to the vacuum

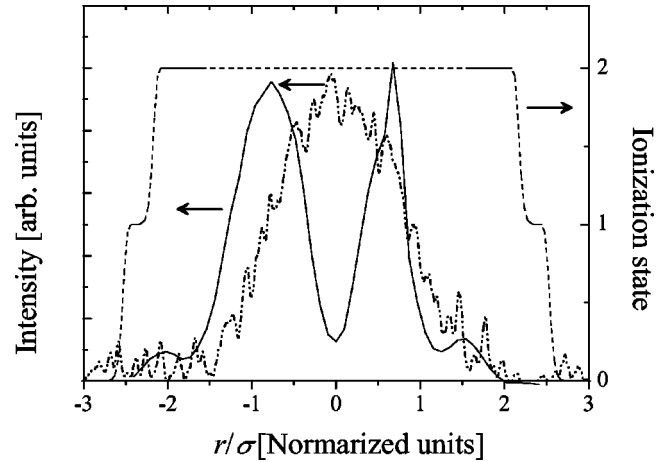


FIG. 2. The dotted line and the solid line correspond to the typical lateral profiles of the pump-laser intensity and the second-harmonic intensity at the focal plane. The peak intensity of the pump pulse at the focal plane was  $5 \times 10^{17}$  W/cm<sup>2</sup>. The broken line is the spatial distribution of the ionization state, which was estimated with the ADK theory for the experimental condition.

spot size, but also the ponderomotive electron cavitation was excited during the pump-pulse duration. The measured oscillation period of the EPW was confirmed to be longer than the pulse width of the pump pulse, then the SRS process never happened, while in the previous [13,14] reports the second-harmonic emission of SRS light was measured.

In the measurement of the second-harmonic emission, we used almost the same setup as that in the measurement of the temporal oscillation of EPW. The second-harmonics emission generated at the plasma was imaged on the charge-coupled device camera with an  $f/4$  doublet, which was set behind the focal point. The pump pulse was reflected before the  $f/4$  doublet by an IR mirror. The second-harmonic emission from plasma was selected with a narrow-bandpass filter centered at 400 nm. The imaging magnification of the second harmonics was  $15\times$ , and the spatial resolution of the imaging system was estimated to be  $1.5 \mu\text{m}$ .

The typical radial profiles of the pump-laser intensity at the focal region and the second-harmonic emission from the plasma are shown in Fig. 2. In this measurement, the electron plasma density was  $1 \times 10^{17}$  cm<sup>-3</sup>. The peak intensity of the pump pulse at the focal plane was  $5 \times 10^{17}$  W/cm<sup>2</sup>. The measured second-harmonic profile had two spatial peaks at  $r/\sigma \sim -0.7$  and  $0.6$ . The polarization of the second-harmonic emission was the same direction as that of the pump pulse. The calculated lateral size of the ionized region at the focal plane using a Ammosov-Delone-Krainov (ADK) theory [18] is simultaneously shown in Fig. 2. In the estimation, the temporal shape of the pump pulse was assumed to be the Gaussian of which the pulse width was 100 fs. The ionization state (broken line) corresponds to the right axis. One can see the two steep density gradients corresponding to the two ionization stages of He gas. In our experimental condition, the lateral size of the fully ionized region was estimated to be  $26 \mu\text{m}$ . The ionization region is much larger than the emis-

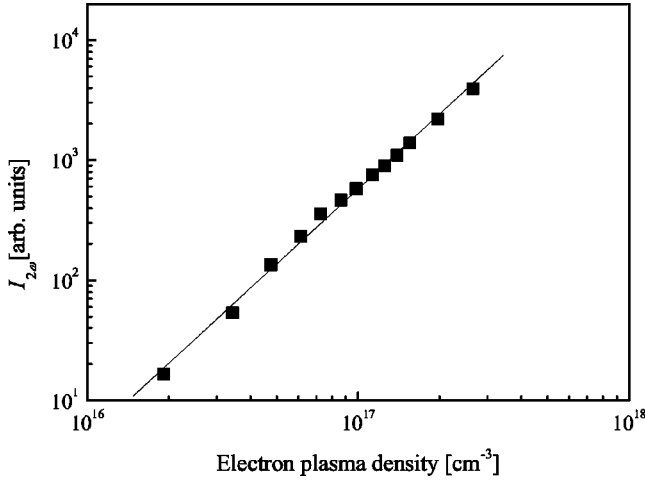


FIG. 3. The second-harmonic intensity versus electron plasma density. The pump intensity was  $5 \times 10^{17}$  W/cm<sup>2</sup>. The dots correspond to the experimental data. The solid line is proportional to the square of the electron density.

sion area of second harmonic. Therefore, the second-harmonic emission was not generated at the edge of the plasma in our case.

Figure 3 gives the intensity of the second harmonics as a function of the electron plasma density. In Fig. 3, the intensity of the pump pulse was  $5 \times 10^{17}$  W/cm<sup>2</sup>, then  $a_0$  was 0.5. The emission intensity of the second harmonic was proportional to the square of the electron plasma density. Moreover, Fig. 4 gives the intensity of the second harmonics as a function of the focused intensity of the pump pulse. The pressure of target gas was fixed to be 1.5 Torr, which corresponds to the electron density of  $1 \times 10^{17}$  cm<sup>-3</sup>. Then the oscillation period of the EPW was estimated to be 350 fs, which is also longer than the pulse width of the pump pulse. The laser intensity was varied with changing the energy of the yttrium aluminum garnet laser which pumps the final amplifier in the TW Ti:sapphire laser system. The intensity of the second-

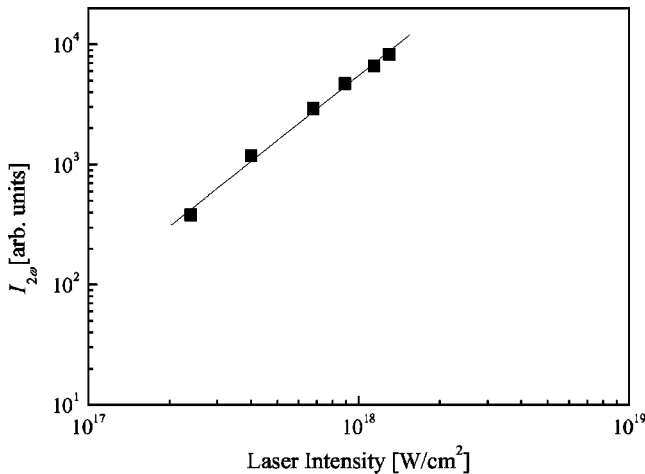


FIG. 4. The second-harmonic intensity versus laser intensity of the pump pulse. The target gas pressure was fixed to be 1.5 Torr. The dots correspond to the experimental data. The broken line is proportional to the laser intensity with the power of 1.8.

harmonic emission was proportional to the laser intensity with the power of 1.8, not proportional to the square of the intensity.

To explain this intensity dependence and spatial profile of the second harmonic, let us consider the mechanism of the second-harmonic generation from the plasma. It was described in Ref. [11], in which the mechanism of the odd-order harmonic generation was precisely explained. Usually, the even-order harmonics are never generated from the uniform plasma. However, as is pointed out in Ref. [11], if the plasma has initial transverse density gradients prior to the arrival of the pump pulse, the second harmonics may be generated. The source current for the second-harmonic emission  $S_{2\omega}$  is proportional to the product of  $\delta n_q \times a$ , where  $\delta n_q$  is the charge perturbation by the quivering electrons and  $a = a_0 \cos \omega t$ , where  $\omega$  is the laser frequency. For estimating  $\delta n_q$ , let us consider the electric field  $E_q$ , which is caused by the quivering electrons.  $E_q = n_0 x$ , where  $n_0$  is the average background electron density and  $x$  is the quiver amplitude. Then,

$$x = \frac{e E_0 \cos \omega t}{m \gamma \omega^2} \propto \frac{a}{\gamma}, \quad (1)$$

where  $\gamma$  is the relativistic parameter,  $E_0$  is the electric field of the laser pulse and  $e$  and  $m$  are the electron charge and mass, respectively. By the Gauss's law,  $\delta n_q = \partial E_q / \partial r$ . Usually  $\partial n_0 / \partial r = 0$ , then  $S_{2\omega} = 0$ . However, if  $\partial n_0 / \partial r \neq 0$ ,

$$S_{2\omega} \propto \frac{a_0^2}{\gamma} \frac{\partial n_0}{\partial r} \cos 2 \omega t. \quad (2)$$

Therefore, the second-harmonic emission may be generated if the plasma has the transverse density gradients. If the scale length of the density gradient by the ponderomotive displacement is assumed to be  $L_p$ ,  $\partial n_0 / \partial r = n_0 / L_p$ . These density gradients become largest at the beam edges. We assumed that they are roughly determined by the laser focal profile and a constant for this set of measurements. Therefore, the power of the second-harmonic emission  $P_{2\omega}$  is proportional to  $a_0^4 / \gamma^2 \times (n_0 / L_p)^2$ . The relativistic parameter  $\gamma$  is given by  $\gamma = \sqrt{1 + a_0^2 / 2}$ , then

$$P_{2\omega} \propto \frac{a_0^4}{1 + a_0^2 / 2} \left( \frac{n_0}{L_p} \right)^2. \quad (3)$$

For example, in the second-harmonic generation with the nonlinear crystal, the motion of electrons that relate to the effective dipole moment is not relativistic, then  $P_{2\omega} \propto I_0^2$ . Only in the plasma, the motion of the electrons is able to become relativistic. By including the relativistic effect, the second-harmonic intensity is proportional to the laser intensity with the power of 1 in  $a_0 \gg 1$ , although it is proportional to the power of 2 in  $a_0 \ll 1$ . In our experimental condition,  $a_0$  was between 0.3 to 0.8, therefore,  $0.1 < a_0^2 (\propto I_0) < 0.65$ . At  $a_0 = 0.7$  ( $a_0^2 = 0.5$ ), the second-harmonic intensity was esti-

mated to be proportional to the laser intensity with the power of 1.8 from Eq. (3). Then, the experimental result is in good agreement with the theory.

As seen in Eq. (2), the spatial profile of the second harmonic depends on the spatial profile of the plasma density gradient and the laser intensity profile. The relativistic effect of quiver motion does not relate at the spatial profile of the second harmonic. In our case, the density gradient is induced by the electron cavitation by the ponderomotive force of the pump-laser pulse.

We observed the second-harmonic emission from the plasma, of which density was low enough to induce no SRS process. By the observation of the dynamics of the EPW, the oscillation period of the EPW in the study was confirmed to be longer than its duration of the pump pulse. Then the second-harmonic emission was generated by the spatially asymmetric nonlinear motion of electrons, which are ex-

pelled from the focal spot by the ponderomotive force. The obtained spatial profile of the second harmonic had two spatial peaks. This spatial profile may be explained by a simple theory. The observed second-harmonic intensity was proportional to the electron plasma density with the power of 2, and proportional to the laser intensity with the power of 1.8. The laser intensity dependence of the second-harmonic intensity may be explained by taking the relativistic effect of electron motion into account.

We would like to acknowledge the technical support of S. Taki and T. Shiraishi. This work was supported by the Research Foundation for Opto-Science and Technology, University of Tsukuba TARA Project, the Grant-in-Aid for Scientific Research by The Japanese Ministry of Education, Science, Sport and Culture.

- 
- [1] M. D. Perry, B. C. Stuart, G. Tietbohl, J. Miller, J. A. Britten, R. Boyd, M. Everett, S. Herman, H. Nguyen, H. T. Powell, and B. W. Shore, in *Conference on Lasers and Electro-Optics*, Vol. 9 of 1996 OSA Technical Digest Series (Optical Society of America, Washington, D.C., 1996), pp. 307–308.
  - [2] K. Yamakawa, M. Aoyama, S. Matsuoka, T. Kase, Y. Akahane, and H. Takuma, *Opt. Lett.* **17**, 1131 (1998).
  - [3] M. Tabak, J. Hammer, M. E. Glinsky, W. L. Kruer, S. C. Wilks, J. Woodworth, E. M. Campbell, and M. D. Perry, *Phys. Plasmas* **1**, 1626 (1994).
  - [4] T. Tajima and J. M. Dawson, *Phys. Rev. Lett.* **43**, 267 (1979).
  - [5] A. McPherson, B. D. Thompson, A. B. Borisov, K. Boyer, and C. K. Rhodes, *Nature (London)* **370**, 631 (1994).
  - [6] E. Takahashi, H. Honda, E. Miura, N. Yugami, Y. Nishida, K. Katsura, and K. Kondo, *J. Phys. Soc. Jpn.* **69**, 3266 (2000).
  - [7] P. Sprangle, E. Esarey, J. Krall, and G. Joyce, *Phys. Rev. Lett.* **69**, 2200 (1992).
  - [8] J. A. Stamper, R. H. Lehmborg, A. Schmitt, M. J. Herbst, F. C. Young, J. H. Gardner, and S. P. Obenschain, *Phys. Fluids* **28**, 2563 (1985).
  - [9] J. Mayer and Y. Zhu, *Phys. Fluids* **30**, 890 (1987).
  - [10] D. Strickland and G. Mourou, *Opt. Commun.* **56**, 219 (1985).
  - [11] E. Esarey, A. Ting, P. Sprangle, D. Umstadter, and X. Liu, *IEEE Trans. Plasma Sci.* **21**, 95 (1993).
  - [12] P. Sprangle, E. Esarey, and A. Ting, *Phys. Rev. A* **41**, 4463 (1990).
  - [13] K. Kruslnick, A. Ting, H. R. Burris, A. Fisher, C. Manka, and E. Esarey, *Phys. Rev. Lett.* **75**, 3681 (1995).
  - [14] V. Malka, A. Modena, Z. Najmudin, A. E. Dangor, C. E. Clayton, K. A. Marsh, C. Joshi, C. Danson, D. Neely, and F. N. Walsh, *Phys. Plasmas* **4**, 1127 (1997).
  - [15] H. Honda, K. Katsura, E. Takahashi, and K. Kondo, *Appl. Phys. B: Lasers Opt.* **70**, 395 (2000).
  - [16] E. Takahashi, H. Honda, E. Miura, N. Yugami, Y. Nishida, K. Katsura, and K. Kondo, *Phys. Rev. E* **62**, 7247 (2000).
  - [17] J. R. Marques, F. Dorchies, F. Amiranoff, P. Audebert, J. C. Gauthier, J. P. Geindre, A. Antonetti, T. M. Antonsen, Jr., P. Chessa, and P. Mora, *Phys. Plasmas* **5**, 1162 (1998).
  - [18] M. V. Ammosov, N. B. Delone, and V. P. Krainov, *Zh. Éksp. Teor. Fiz.* **91**, 2008 (1986) [*Sov. Phys. JETP* **64**, 1191 (1986)].